Available online at www.sciencedirect.com
SCIENCE DIRECT®
Proceedings of the Combustion Institute 30 (2005) 2701–2709
Proceedings of the Combustion Institute
www.elsevier.com/locate/proci

Combustion timing in HCCI engines determined by ion-sensor: experimental and kinetic modeling

P. Mehresh[a,*], J. Souder[a], D. Flowers[b], U. Riedel[c], R.W. Dibble[a]

[a] *Combustion Analysis Laboratory, University of California, Berkeley, CA 94720, USA*
[b] *Lawrence Livermore National Laboratory, Livermore, CA 94551, USA*
[c] *Interdisciplinary Center for Scientific Computing, University of Heidelberg, Germany*

Abstract

The ion current signal in homogenous charge compression ignition (HCCI) engines is studied. The aim of this research is to show that a measurable ion current exists even in the very lean combustion (equivalence ratio $\phi = 0.35$) in an HCCI engine. Numerical models using detailed chemical kinetics for propane combustion, including kinetics for ion formation, support the experimental findings. The effects of the equivalence ratio, the intake mixture temperature, and the applied bias voltage on the ion signal are studied through a series of experiments. The findings are compared to the numerical model results. The research shows that an inexpensive ion sensor may replace the expensive pressure transducers currently used in HCCI engines. The ion current signal is very sensitive to the equivalence ratio of the intake fuel–air mixture. Through numerical modeling, the N_2O mechanism is shown to be the significant source of Nitrogen Oxides (NO_x) generation in HCCI combustion.

Keywords: HCCI; Modeling; Ion sensor; NO_x; Flame ionization

1. Introduction

1.1. HCCI technology

The homogeneous charge compression ignition (HCCI) engine has received renewed interest in recent years. In the past decade, several hundred papers have been published, largely in the Society of Automotive Engineers literature. A recent publication reviews much of this literature [1]. HCCI engines have features of both spark ignited (SI) and diesel engines. HCCI engines are generally premixed like SI engines, but operate much leaner ($\phi < 0.5$) than SI engines (typically $\phi \sim 1$). Lean combustion implies lower peak cylinder temperatures and therefore lower NO_x. These lean mixtures also have low particulate emissions. HCCI engines typically have high compression ratios, like diesel engines, which result in their high efficiencies. In a SI engine, a spark initiates the combustion event, and the spark timing is routinely adjusted. Similarly, the injection of diesel fuel initiates the combustion event in a diesel engine. However, the HCCI engine does not have a spark plug or direct fuel injection. The combustion event occurs when the cylinder contents are hot enough (e.g., ~1200 K) for a long enough period of time (e.g., ~3 ms). Here, CA50 is defined as the engine's crank angle position where 50% of the

* Corresponding author. Fax: +1 510 642 1850.
E-mail address: pmehresh@me.berkeley.edu (P. Mehresh).

1540-7489/$ - see front matter
doi:10.1016/j.proci.2004.08.135

cumulative heat release is achieved. As the initiation of combustion depends largely on the chemistry and the conditions (particularly temperature) inside the cylinder, controlling HCCI combustion timing is a major challenge. The control process involves three steps: a signal is sensed, the signal is processed, and something is actuated. Of the three steps, the processing is most readily accomplished, using microprocessors and either "look-up" tables or more involved control system techniques.

There are many proposed actuation strategies for controlling HCCI combustion timing. One strategy adds various amounts of ozone to the intake [2]. Another strategy injects pilot fuel during the negative overlap between the exhaust and intake valves, which varies the conditions at the start of the main combustion and thus CA50 [3]. Other strategies include using a variable compression ratio engine achieved via late intake valve closure like in Atkinson cycle-based engines [4], using a variable compression ratio engine affected by "beam" designs [5], blending hot and cold intake air to control the inlet air temperature [6], and blending high cetane number fuels with low cetane number fuels [7].

To implement the above control strategies, the CA50 event must be sensed. For research purposes, detecting CA50 is usually done with a piezoelectric pressure transducer. The piezoelectric pressure transducer is considered too expensive and too fragile for a mobile engine's routine environment. Various other sensors have been proposed. These include sensors that can detect acoustics (a.k.a. "knock") from the combustion chamber, torque transducers that can detect pressure pulses [8], sensors to detect light emissions from the combustion event [9], and ion sensors which detect the ion current associated with a gasoline-fueled HCCI engine [10]. This paper explores the use of an ion sensor to determine CA50 in a propane-fueled HCCI engine. A numerical model of the chemical kinetic production of ions in HCCI combustion is also developed.

1.2. Ionization in flames

The fact that flames produce ions and are thus weak plasmas has been known for a long time. The first scientific inquiries into the subject of ions in flames "… were laid as early as 1600 when W. Gilbert, physician to Queen Elizabeth I, demonstrated that flame gases would discharge an electroscope" [11]. The texts by Lawton and Weinberg [12] and Gaydon [13] contain early discussions on ions in flames. Fialkov [14] provides a more recent review of the subject. Ion concentrations in the range of 10^9–10^{12} ions-cm^{-3} are reported in hydrocarbon/air flames, with the highest concentrations occurring when acetylene is the fuel [12]. The Saha equation can be used to calculate the ion density and the electron density in thermodynamic equilibrium. Investigations show that the ion concentrations in flames are far in excess of what equilibrium predicts [15]. In fact, ions owe their origin to chemical kinetics processes occurring in the reaction zone. Calcote [16] and Brown [17] give the principal source of ions in hydrocarbon flames as the chemi-ionization reaction

$$CH + O \rightarrow CHO^+ + e^- \quad (1)$$

followed rapidly by the charge exchange reaction

$$CHO^+ + H_2O \Longleftrightarrow H_3O^+ + CO \quad (2)$$

H_3O^+ is the dominant ion in both lean and slightly rich hydrocarbon flames. The dominant ion becomes $C_3H_3{}^+$ only in very rich and near-sooting flames [17,18].

Langmuir probes, microwave absorption, and ion-mass spectrometers are some of the experimental tools for investigating ions in flames. When an electric field is applied across the reaction zone in a flame, a current flows through the circuit due to the presence of ions and electrons (here, ions mean positively charged molecular species, e.g., H_3O^+). This is called an ion current and is affected by ion density, gas flow, flame geometry, electric potential, and the angle between the flame and electrode [19]. Tomita and co-workers [20–22] have used ion probes of different types to sense the ion current produced during combustion in SI engines. The effect of NO addition on autoignition was also reported using an ion current sensor [23].

1.3. Ion sensor technology

In general, expensive pressure transducers are used in laboratories to determine combustion characteristics in the engine. Ion sensors are significantly less expensive than pressure transducers. For example, an existing spark plug can often be used as an ion sensor. An ion sensor signal has been used for combustion diagnostics [20–22], combustion stability control [24], peak pressure position control [25], and predicting mass fraction burned [26] in SI engines. Many publications report the efficacy of an ion current signal in the prediction of knock onset in SI engines [9,23,27]. Even the engine on the venerable Harley–Davidson motorcycle has a spark plug that, right after emitting a spark, switches circuitry and becomes an ion sensor, sensing for the onset of engine knock. The engines cited above operate at or near stoichiometric conditions where temperatures are high and the production of chemi-ions is significant. As engines operate leaner, the lower temperatures dramatically reduce the production of chemi-ions. In the case of HCCI engines, where ϕ is seldom above 0.5, few researchers expected to find an ion signal. However, a recent paper has been the first to report an ion signal in a gasoline-fueled HCCI engine [10].

Present work explores the chemical kinetic origins of the ion signal in a propane-fueled HCCI engine. The ion signal in an HCCI engine is experimentally investigated, and the ion generation is numerically modeled. A single zone numerical model containing ion chemistry is developed to corroborate the experimental results. The intake temperature, equivalence ratio, and bias voltage effects on the ion signal is reported.

Nitrogen oxides in the atmosphere contribute to photochemical smog, acid rain precursors, the destruction of the ozone in the stratosphere, and global warming [28]. The NO_x in hydrocarbon fuel combustion is generated by three different mechanisms: the Zeldovich or thermal mechanism [29], the N_2O mechanism [30,31], and the Fenimore or Prompt NO_x mechanism [32]. Various studies have been carried out to understand the relative importance of these three mechanisms in the formation of the total NO_x in various combustors, such as internal combustion engines [33] and gas turbines [34]. In a SI engine where the flame temperature is high (typically ~2700 K), results show that the Zeldovich mechanism contributes the most to total NO_x. The N_2O mechanism contributes significantly to total NO_x in a "low temperature, high pressure" type combustion, which is typical of lean pre-mixed gas turbines.

Since HCCI engines work on extremely lean mixtures, the typical flame temperature is around 1900 K. Due to high compression ratios, the pressure inside the combustion chamber in an HCCI engine is somewhat higher than SI engines. The NO_x generation in HCCI engines, although not significant given the low amount of NO_x generated (typically 2–5 PPM), is also examined in this paper using numerical models.

2. Experimental set-up and methods

The experiments are performed on a 4-cylinder, 1.9L Volkswagen TDI engine converted to run in HCCI mode. The specifications of the engine are given in Table 1. The ion sensor circuit is shown in Fig. 1. The engine block acts as the positive electrode. The ion-sensor is mounted in the glow plug hole of cylinder 1, and its center electrode (negative) is insulated from the engine block. AVL QH33D piezoelectric pressure transducers are mounted in injector holes to capture the cylinder pressure. National Instruments Labview 'Visual Instruments' programs are used to monitor the low speed data and a Mathworks' Matlab program monitors and collects the high speed cylinder pressure and ion signal data. A series of experiments are performed with variations in the equivalence ratio, the intake temperature of the fuel–air mixture, and the bias voltage applied across the two electrodes of the ion-sensor.

Table 1
Engine specifications

Displacement	1.9 L
Cylinder bore	79.5 mm
Stroke	95.5 mm
Connecting rod length	144.0 mm
Compression ratio	19:1
Firing order	1-3-4-2
Engine speed	1800 rpm
IVO	16 ATDC
IVC	25 ABDC
EVO	28 BBDC
EVC	19 ATDC

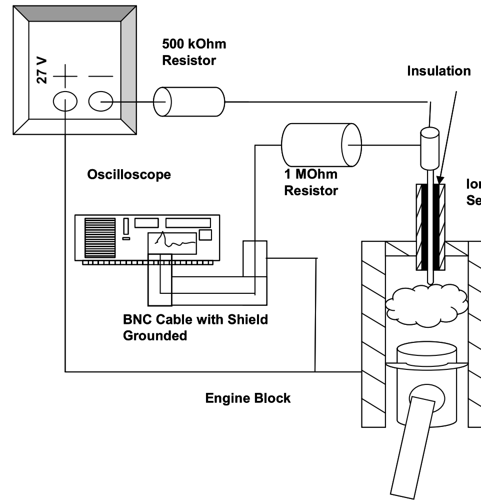

Fig. 1. Schematic of an ion sensor in an HCCI engine.

Propane is used as a fuel for all the experiments unless otherwise stated. A Sierra Instruments 810 series mass flow controller is used to accurately control the fuel flow rate. Thermocouples are mounted in the intake ports of each cylinder to measure the intake temperature of the fuel–air mixture. Bias voltages of 27, 54, and 90 V are used. Regular 9 V batteries supply the necessary bias voltage since the current required in the circuit is very low.

3. Numerical model

Simulations of HCCI combustion and the ion-generation are conducted using a single-zone model of the engine. This model treats the combustion chamber as a spatially uniform reactor with time-dependent temperature, pressure, and composition. Conservation of energy and chemical kinetic relations based on a gas-phase detailed kinetic mechanism for propane combustion are

Table 2
Rate coefficients of major ionization reactions

	Reaction	A (cm mol s)	β (—)	E_a (kJ/mol)	Ref.
1	$CH + O \rightarrow CHO^+ + e^-$	4.600E + 08	0.73	−2.6	[16]
2	$CHO^+ + e^- \rightarrow CO + H$	1.325E + 17	0.00	0.0	[37]
3	$CHO^+ + H_2O \rightarrow H_3O^+ + CO$	1.000E + 16	−0.09	0.0	[17]
4	$H_3O^+ + e^- \rightarrow H_2O + H$	2.291E + 18	−0.50	0.0	[17]
5	$H_3O^+ + e^- \rightarrow OH + H + H$	7.949E + 21	−1.37	0.0	[38]

solved to determine temperature and species histories for the cycle.

The main chemical kinetic mechanism is the well-known detailed Warnatz mechanism. This mechanism C–H–N–NO (C1–C4 chemistry) has been validated in numerous simulations documented in the literature. The Warnatz mechanism is then augmented with a skeletal ion formation and consumption mechanism. Our ionization model contains 34 reactions involving 9 ionic species (NO^+, N^+, $N_2{}^+$, $O_2{}^+$, OH^+, O^+, H_3O^+, HCO^+, and electron). By far, the five most dominant reactions are presented in Table 2. These reactions focus on the formation and consumption of H_3O^+ as the main ion species [35]. The initiation reaction for ionization is reaction (R1) in Table 2 [17], which leads to the formation of CHO^+. Here, the rapid formation of H_3O^+ in the CHO^+ reaction with water (R3) is considered as well as $H3O^+$ consumption in the neutralization reactions (R4, R5). Furthermore, reaction (R2) accounts for the loss of CHO^+ in the neutralization reaction with electrons. It will be shown that reactions of higher hydrocarbons with ions are not needed for good agreement between the model and experiments.

The reactor volume is given by slider–crank relations that determine the motion of the piston in the cylinder. The simulation handles only the closed part of the cycle; intake and exhaust processes are not considered. The single-zone model is a highly idealized representation of the actual processes occurring in the combustion chamber. More detailed models exist that capture the three-dimensional processes occurring in the combustion chamber, such as crevice and boundary layer effects. However, single-zone models can give insight into the processes occurring in the combustion chamber. This is especially true for processes that occur in the hottest central core gases of the combustion chamber, away from the crevice and boundary layers.

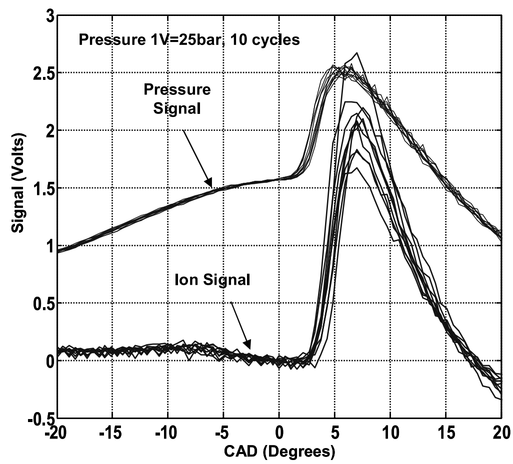

Fig. 2. Ion signal (volts × 100) and pressure transducer signal (1 V = 25 bar) for 10 consecutive cycles, $\phi = 0.38$.

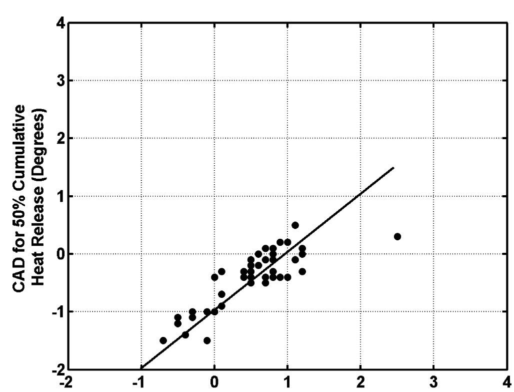

Fig. 3. Linear relationship between CA50 and CAD for 50% ion signal. Experimental results.

4. Results and discussion

Figure 2 show pressure and ion signal data for several consecutive cycles. The ion signal is easily seen. Figure 3 shows a correlation between the pressure and ion signal. Such a correlation allows for the estimation of CA50 using the ion signal. Recall that CA50 is usually determined by an expensive pressure transducer.

Figure 4 shows the pressure and ion concentrations predicted by the numerical model. It is well known that a single zone model of HCCI captures the main features but over-predicts the rate of pressure rise and the rise in ion concentration. Figure 5, the numerical analog of Fig. 3, shows

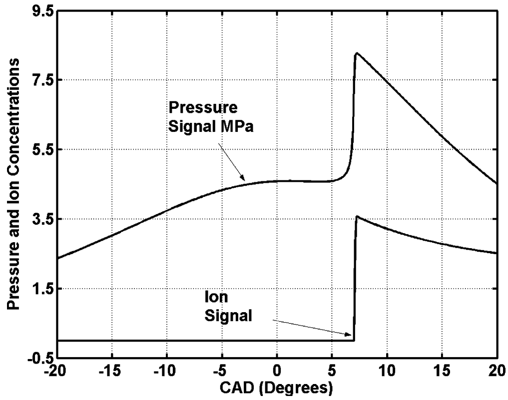

Fig. 4. Numerical model predictions of pressure inside the cylinder (MPa) and ion concentration (mol/ (5×10^{12})).

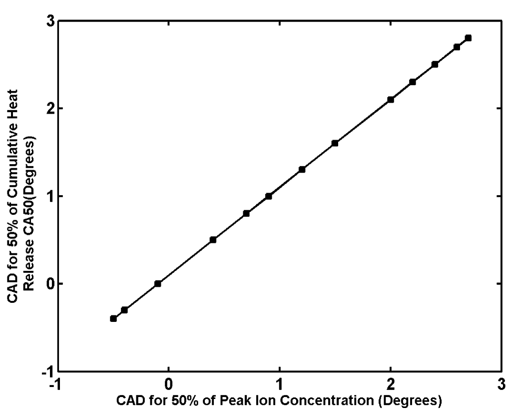

Fig. 5. Numerical model predictions of the correlation between CA50 and CAD for 50% ion concentration peak. The fitted line shows a linear relationship, similar to the experimental results shown in Fig. 3.

that the ion signal is a suitable measure of CA50 and thus could be used for feedback control of HCCI engines. A careful examination of the two figures leads to the conclusion that the CA50 estimated from the 50% ion concentration has a 1-degree delay. The RC time constant of the ion-circuit is responsible for the delay. Experiments conducted with various resistor values shows a corresponding change in the ion signal delay. Mathematical models of the ion sensor and its wiring harness lead to the same conclusion. The ion sensor acts as a capacitor in the circuit. The ion pulse causes a current to flow through the circuit and that pulse can be modeled as a current source. The differential equation representing the circuit diagram (see Fig. 6) is

$$\dot{V}_C = \left[-\frac{1}{RC}\right]V_C + \frac{1}{C}i_S - \frac{1}{RC}V_S, \tag{3}$$

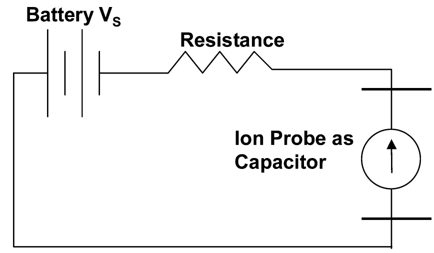

Fig. 6. A simplified diagram of the circuit used to model the ion signal delay.

where V_C is the voltage across the capacitor (ion sensor), V_S is the battery voltage, and i_S is the current flow due to the ion pulse. The ion current is simulated using a Gaussian input pulse with a peak magnitude of 1. R and C are the resistance in the circuit and capacitance of the ion sensor, respectively. Two different resistances values are used to demonstrate the effect of the RC time constant on the ion signal delay. Figures 7 and 8 show the experimentally measured and model-predicted effects of the RC time constant on the ion signal delay, respectively.

Figure 9 shows the dependence of the experimental ion-signal on the equivalence ratio for propane. The ion signal increases rapidly with increasing equivalence ratios. At $\phi \sim 0.32$ for propane, the measured ion signal becomes unusable as the signal-to-noise ratio approaches one. This lower value of equivalence ratio is expected to be a function of the fuel used. As already mentioned, the main ion generation reaction is the chemi-ionization reaction which is initiated by the presence of CH radicals. Hence, the fuels

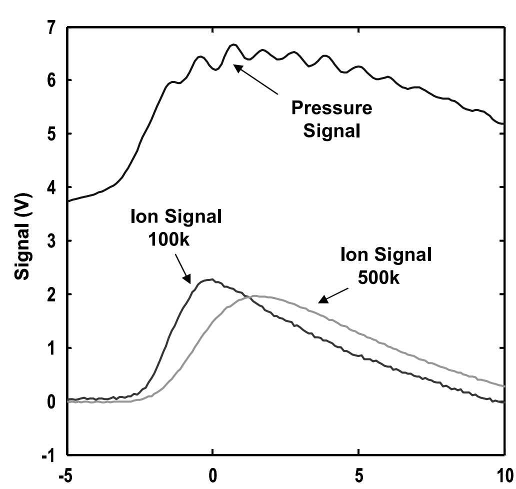

Fig. 7. Experimental results show the ion signal (volts∗100) and pressure transducer signal (1 V = 10 bar) for two different resistances in series with the ion sensor. The change in signal delay is evident.

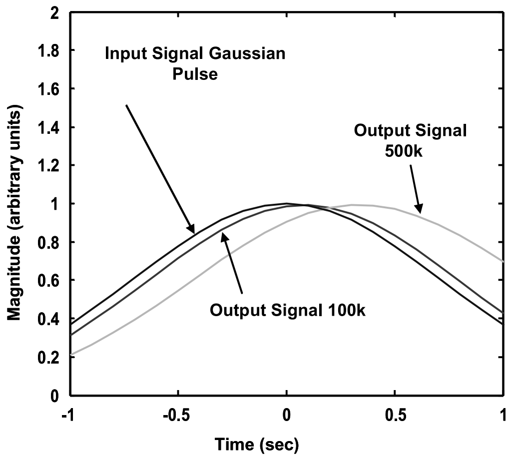

Fig. 8. Model results for 2 different resistances in series with the ion sensor (modeling the schematic in Fig. 6). The change in signal delay is evident.

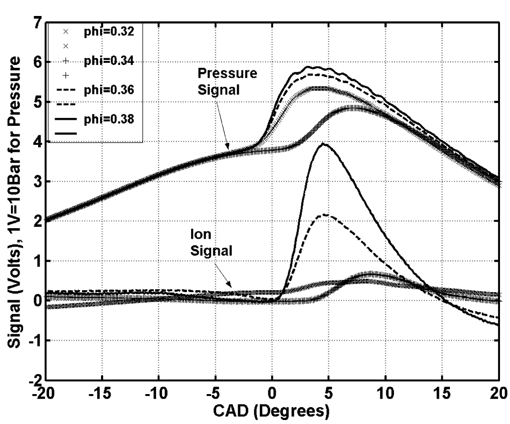

Fig. 9. Experimental results showing a strong dependence of ion-signal on the equivalence ratio. Propane is used as the fuel for above experiments.

which produce lots of CH radicals should produce higher ion concentrations and a better ion signal. Figure 10 shows how the model predictions compare to the measured ion signal as the equivalence ratio is increased. The model predictions capture the experimental trend and show that the ion signal rapidly increases with increasing ϕ.

Figure 11 shows the numerical predictions of the ion concentration as a function of peak cycle temperature. The large increase in ion concentration with increasing temperatures is the reason ion sensors work well in SI ($\phi \sim 1$) and diesel engines (where there is a stoichiometric contour resulting in temperatures as high as 2700 K). Such stoichiometric temperatures are significantly higher than the temperatures in Fig. 11. At the peak HCCI combustion temperature (typically $T \sim 1900$ K), the ion concentration is relatively low. In spite of the

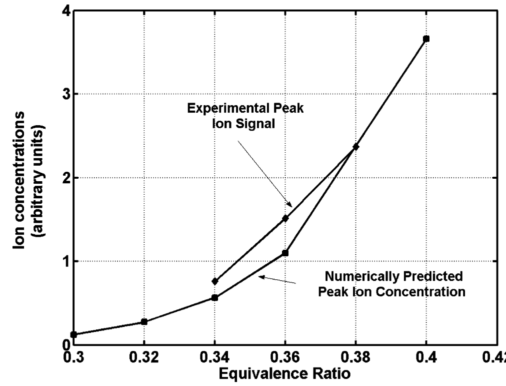

Fig. 10. Comparison of experimental data and model predictions of the variation of ion signal with ϕ. The maximum value of the ion signal is plotted with maximum concentration predictions from the model.

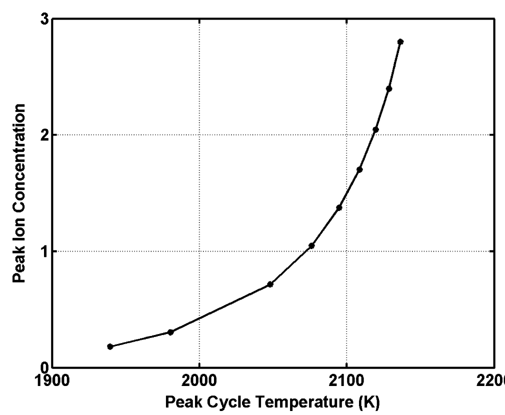

Fig. 11. Numerical model predictions of the ion concentration plotted against the peak cycle temperature.

low concentration, the ion signal is adequate for feedback control of an HCCI engine.

The effect of the bias voltage applied to the ion circuit on the ion signal is also experimentally investigated. The bias voltage does affect the peak value of the signal, but the signal-to-noise ratio remains the same for the cases studied.

5. NO_x generation in HCCI

The text by Warnatz et al. [36] has a review of NO_x generation in hydrocarbon combustion. Although little NO_x is generated in HCCI engines, it is important to understand the underlying phenomenon. As already mentioned, the peak temperature in a typical HCCI combustion event is around 1900 K. It is well established that the NO_x generation is a strong function of temperature. Also, the three different NO_x generation mechanisms depend differently on the temperature and pressure during the combustion. To identify

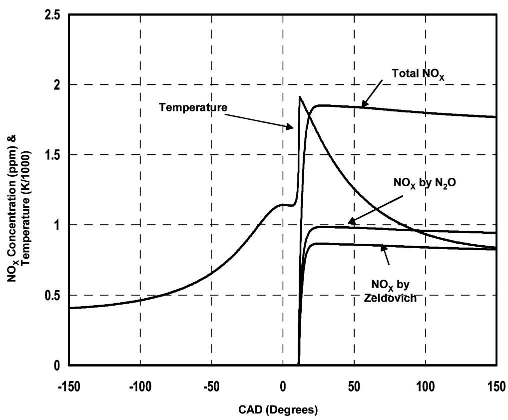

Fig. 12. The numerical model of HCCI combustion shows unusual situations. The contribution of the N_2O mechanism in NO_x generation is higher than the contribution of the thermal mechanism. The maximum temperature in the cycle is 1900 K, $\phi = 0.3$. Fenimore mechanism's contribution is insignificant.

the relative importance of the three mechanisms in HCCI combustion, numerical simulations are used. The total NO_x is first calculated using the complete mechanism. Then, the reactions relevant to the Fenimore mechanism are removed from the complete mechanism and the NO_x generated is calculated again. The difference between the total NO_x and the NO_x calculated with the Fenimore reactions removed is identified as the contribution of the Fenimore reactions to the total NO_x. Similar procedure is adopted for the N_2O and Zeldovich mechanisms to obtain their respective contributions. Figure 12 shows the results. The start of combustion and the intake conditions are held constant for each simulation. It is evident from Fig. 12 that for the low temperature and high pressure combustion in HCCI engines, the contribution of the N_2O route of NO_x production is comparable to the thermal or Zeldovich route. The N_2O route contribution to the total NO_x is more than the thermal route contribution for the case shown in Fig. 12.

6. Conclusions

The most important results presented in this paper are summarized as follows:

1. An ion sensor signal was observed in a propane-fueled HCCI engine. The ion sensor can be used in place of the expensive pressure transducers currently used in research engines. The ion sensor is equally capable of capturing cycle-to-cycle variations in HCCI combustion.
2. A numerical model using detailed chemistry (including ionic species) was developed for HCCI combustion and used to predict the ion concentration in the cylinder.
3. The model results were in good agreement with the experimental findings. The effects of equivalence ratio and intake temperature on the ion signal were studied both experimentally and numerically. The ion signal becomes stronger with increases in equivalence ratio and intake temperature.
4. Due to the low temperature and high pressure HCCI combustion, the N_2O mechanism contributes significantly to the total NO_x production. In some cases, the N_2O route produces more NO_x than the Zeldovich route.

Acknowledgments

This research was supported by the DOE, Award No. F006635, A University Consortium on HCCI Engine Research (P.M., J.S., R.W.D.) and the DOE/LLNL, Award No. B530482, Low Cost, High Efficiency, Ultra-Low NO_x, ARICE Solution Using HCCI Combustion (DF).

References

[1] F. Zhao, *Homogeneous Charge Compression Ignition (HCCI) Engines: Key Research and Development Issues*, SAE International, USA, 2003.

[2] P.F. Flynn, G.L. Hunter, A.O. zurLoye, O.C. Akinyemi, R.P. Durrett, G.A. Moore, J.M. Mudd, G.G. Muntean, J.A. Wagner, J.F. Wright, *Premixed Charge Compression Ignition Engine with Optimal Combustion Control*. U.S. Patent No.: US6286482 B1, 2001.

[3] L. Koopmans, R. Ogink, I. Denbratt, *Direct Gasoline Injection in Negative Valve Overlap of a Homogeneous Charge Compression Ignition Engine*. SAE 2003-01-1854, 2003.

[4] R. Stone, *Introduction to Internal Combustion Engines*, third ed., SAE International, USA, 1999.

[5] Freudenstein, Ferdinand, Sohn, J. Wayne, *Swing Beam Internal Combustion Engines*. U.S. Patent No., US4917066, 1990.

[6] J. Yang, T. Culp, T. Kenney, *Development of a Gasoline Engine System Using HCCI Technology—The Concept and the Test Results*. SAE 2002-01-2832, 2002.

[7] R.H. Stanglmaier, T.W. Ryan III, J.S. Souder, *HCCI Operation of a Dual-Fuel Natural Gas Engine for Improved Fuel Efficiency and Ultra-Low NO_x Emissions at Low to Moderate Engine Loads*. SAE 2001-01-1897, 2001.

[8] D. Taraza, N.A. Henein, W. Bryzik, *Determination of the Gas Pressure Torque of a Multicylinder Engine from Measurements of the Crankshaft's Speed Variation*. SAE 980164, 1998.

[9] T. Suzuki, H. Ohara, A. Kakishima, K. Yoshida, H. Shodi, *A Study of Knocking Using Ion Current and Light Emission*. SAE 2003-32-0038, 2003.

[10] P. Strandh, M. Christensen, J. Bengtsson, R. Johansson, A. Vressner, P. Tunestal, B. Johansson,

Ion Current Sensing for HCCI Combustion Feedback. SAE 2003-01-3216, 2003.
[11] F.J. Weinberg, *Advanced Combustion Methods*, Academic Press (London), UK, 1986, p. 334.
[12] J. Lawton, F.J. Weinberg, *Electrical Aspects of Combustion*, Clarendon Press, UK, 1969.
[13] A.G. Gaydon, H.G. Wolfhard, *Flames Their Structure Radiation and Temperature*, fourth ed., Halsted Press, USA, 1979, pp. 340–370.
[14] A.B. Filakov, *Progr. Energy Combust. Sci.* 23 (1997) 399–528.
[15] J.M. Goodings, D.K. Bohme, T.M. Sugden, *Proc. Combust. Inst.* 16 (1976) 891–902.
[16] H.F. Calcote, R.J. Gill, *Development of the kinetics for an ionic mechanism of soot formation in flames*, Eastern section of the Combustion Institute, Fall Technical Meeting, 1994.
[17] R.C. Brown, A.N. Eraslan, *Combust. Flame* 73 (1) (1988) 1–21.
[18] B. Lewis, G. von Elbe, Combustion*, Flames and Explosions of Gases*, third ed., Academic Press, USA, 1987, p. 423, 579.
[19] T. Suzuki, Y. Hashimoto, I. Mashiko, T. Hirano, *Combust. Flame* 36 (1979) 179–191.
[20] S. Yoshiyama, E. Tomita, Y. Homamoto, *Fundamental Study on Combustion Diagnostics Using a Spark Plug as Ion Probe*. SAE 2000-01-2828, 2000.
[21] S. Yoshiyama, E. Tomita, *Combustion Diagnostics of a Spark Ignition Engine Using a Spark Plug as an Ion Probe*. SAE 2002-01-2838, 2002.
[22] S. Yoshiyama, E. Tomita, N. Tabuchi, K. Matsumoto, K. Matsuki. *Combustion Diagnostics of a Spark Ignition Engine by Using Gasket Ion Sensor*. SAE 2003-01-1801, 2003.
[23] O. Stenlaas, P. Einwall, R. Egnell, B. Johansson, *Measurement of Knock and Ion Current in a Spark Ignition Engine with and without NO Addition to the Intake Air*. SAE 2003-01-0639, 2003.
[24] I. Andersson, L. Eriksson, *Ion Sensing for Combustion Stability Control of a Spark Ignited Direct Injected Engine*. SAE 2000-01-0552, 2000.
[25] M. Hellring, U. Holmberg, *A Comparison of Ion Current Based Algorithms for Peak Pressure Control.* SAE 2001-01-1920, 2001.
[26] C.F. Daniels, G.G. Zhu, J. Winkelman, *Inaudible Knock and Partial-Burn Detection Using In-Cylinder Ionization Signal*. SAE 2003-01-3149, 2003.
[27] Y. Lee, S. Pae, K. Min, E.S. Kim, *Proc. Inst. Mechan. Eng.* 214 (D) (2000).
[28] D.M. Golden, *Proc. Combust. Inst.* 28 (2000) 2383–2392.
[29] Y.B. Zeldovich, *Acta Physiochem. URSS* 21 (1946) 577.
[30] J. Wolfrum, *Chem. Ing. Tech.* 44 (1972) 656.
[31] P.C. Malte, D.T. Pratt, *Combust. Sci. Technol.* 9 (1974) 221.
[32] C.P. Fenimore, *Proc. Combust. Inst.* 3 (1971) 373.
[33] M.C. Drake, R.J. Blint, *Combust. Sci. Technol.* 75 (1991) 261–285.
[34] S. Correa, *Combust. Sci. Technol.* 87 (1992) 329–362.
[35] H.F. Calcote, *Proc. Combust. Inst.* 9 (1963) 622.
[36] J. Warnatz, U. Mass, R.W. Dibble*, Combustion*, third ed., Springer Press, Germany, 2001.
[37] B.R. Rowe, J.C. Gomet, A. Canosa, C. Rebrion, J.B.A. Mitchell, *J. Chem. Phys.* 96 (2) (1992) 1105–1110.
[38] J. Guo, J.M. Goodings, *Chem. Phy. Lett.* 329 (5 and 6) (2000) 393–398.

Comments

Philippe Dagaut, CNRS-LCSR, France. Your modeling indicates NO is mainly formed via the "N_2O-mechanism." Although this is an expected result under high-pressure and fuel-lean conditions, I would like to know how:

1. The pressure dependence of the reaction $N_2 + O + M \rightarrow N_2O + M$ was handled in the model.
2. The degree of uncertainty for the kinetics of this reaction under your high-pressure conditions.

Reply. 1. As our Conclusions indicate, we choose the word "significant" and not "Mainly." Under some conditions the N_2O mechanism produced less than half of the NO and in some conditions more than half of the NO. Thus we use the word significant. We are dealing with the pressure dependence of the reaction $N_2 + O + M \rightarrow N_2O + M$ by using the following coefficients and kinetic data:

$$K_f = [7.91000E + 010, 0, 56020]$$

$$K_{f0} + [6.37000E + 014, 0, 56640]$$

Efficiencies = "AR:0.625 C_2H_6:3 CH_4:2 CO:1.5 CO_2:2 H_2:2 H_2O:6

2. Reference [1] provides uncertainties in the rate constant. Within the limits of those uncertainties, there is no change in our Conclusion: "...the N_2O mechanism contributes significantly to the total NO_x production."

Source of the kinetic Data are:

References

[1] M. Rohrig, E.L. Petersen, D.F. Davidson, R.K. Hanson, *Int. J. Chem. Kinet.* 28 (1996) 599.
[2] J.E. Johnsson, P. Glarborg, K. Dam-Johansen, *Proc. Combust. Inst.* 24 (1992) 917.

•

Ben Chorpening, US DOE – National Energy Technology Laboratory, USA. In our experience at NETL on ion sensor development for gas turbines, we have observed [1] higher ion currents using positively charged electrodes. Have you evaluated using a positively charged ion sensor in this application, instead of a negatively charged sensor?

Reference

[1] J.D. Thornton, D.L. Straub, G.A. Richards, R.S. Nutter, E. Robey, *"An In-Situ Monitoring Technique for Control and Diagnostics of Natural Gas Combus-*

tion Systems'', 2nd Joint Meeting of the U.S. Sections of the Combustion Institute, Oakland, CA, March 25–28, 2001.

Reply. Several researchers have suggested we may obtain larger signals by reversing polarity of our ion sensor; a recent paper illuminates this for SI engines [1]. The negatively charged ion electrode is an artifact or our adaptation of a glow plug as ion sensor. Our ion sensor works as glow plug when positively charged. This design limitation is being removed and we will explore the effect of polarity on ion-sensor.

Reference

[1] S. Yoshiyama, E. Tomita, Y. Hamamoto, *Fundamental Study on Combustion Diagnostics Using a Spark Plug as Ion Probe*, SAE-2000 01, p. 2828.